Applied Mechanics and Materials *Online: 2012-03-27*
ISSN: 1662-7482, Vol. 162, pp 413-422
doi:10.4028/www.scientific.net/AMM.162.413

Performance Criteria to Evaluate a Kinematically Redundant Robotic Cell for Machining Tasks

Subrin Kévin[1,a], Sabourin Laurent[1,b] , Gogu Grigore[1,c] and Mezouar Youcef[1,d]

[1]Clermont Université, Pascal Institute, UMR 6602 CNRS/UBP/IFMA, BP10448, F-63000 Clermont-Ferrand, France

[a]kevin.subrin@ifma.fr, [b]laurent.sabourin@ifma.fr, [c]grigore.gogu@ifma.fr, [d]youcef.mezouar@lasmea.univ-bpclermont.fr

Keywords: Machining, kinematic redundancy, closed-loop architecture

Abstract. Machine tools and robots have both evolved fundamentally and we can now question the abilities of new industrial robots concerning accurate task realization under high constraints. Requirements in terms of kinematic and dynamic capabilities in High Speed Machining (HSM) are increasingly demanding. To face the challenge of performance improvement, parallel and hybrid robotic architectures have emerged and a new generation of industrial serial robots with the ability to perform machining tasks has been designed. In this paper, we propose to evaluate the performance criteria of an industrial robot included in a kinematically redundant robotic cell dedicated to a machining task. Firstly, we present the constraints of the machining process (speed, accuracy etc.). We then detail the direct geometrical model and the kinematic model of a robot with closed chain in the arm and we propose a procedure for managing kinematic redundancy whilst integrating various criteria. Finally, we present the evolution of the criteria for a given trajectory in order to define the best location for a rotary table and to analyze the manipulator's stiffness.

Introduction

Machine-tools and robots have changed fundamentally in recent years due to the industrial context. Requirements in terms of adaptability, productivity or quality are increasingly important. This has led to the emergence of reconfigurable machine tools, hybrid and parallel robots but also the development of a new generation of industrial robots, more suitable for machining operations.
This article presents their performance in machining applications. We first outline the problem posed and we explain the advantages of using kinematic redundancy to improve kinematic capacity and accuracy. In order to draw attention to the algorithm we have developed to optimize the trajectory, we present the direct geometric model and the Jacobian of a robot with closed chain in the arm. We then present the evolution of the criteria to establish the best location for a rotary table as well as the best posture for the manipulator when conducting stiffness analysis.

Serial robot performance and its improvement

Nowadays, the use of industrial robots for machining tasks is still limited to soft materials (resin, plaster). In fact, the cutting phenomenon causes diverse loading of variable amplitude, frequency and direction. The lack of static and dynamic stiffness of a serial architecture results in structural deformation and causes tool vibration, leading to geometrical defects. The process capability limits highlight the low variable stiffness around 1N/μm [1,2], their first natural frequency between 10Hz and 30Hz [1,3] and the temperature influence on absolute accuracy [4]. The need to reduce investment while increasing productivity pushes manufacturers to invest in new processes and they expect industrial robots to perform accurate tasks. However, in 2005, Summers et al. tried to machine aeronautical parts with an accuracy of 0.2mm without modifying the control [5]. The objective was not achieved and pushed by the industrial context, robot manufacturers were forced to improve their offer. Today, these improvements can be seen in the integration of more powerful motors, stiffer gearboxes limiting vibration phenomena, and generally architectures dedicated to machining (e.g. use of parallelogram loops in the arm (Fig. 2b), integration of the spindle on the fifth axis, etc...). Currently, absolute accuracy is around 0.1mm to 0.2mm, the repeatability is 0.07mm, with a torque of 500Nm on the wrist axes and angular velocities exceeding 100°/s with a maximum payload superior to 150kg. With a cost reduction of 75% in comparison with 5 axis machine tools, the new serial robot presents a better adaptability. In order to improve machining accuracy, one method is to introduce and manage kinematic redundancy thus optimizing cell behavior.

Kinematic redundancy

Redundancy has given rise to many optimization studies. In fact, adding an axis may enable both enlargement of the workspace and obstacle avoidance whilst maintaining a space where specific performances are expected. The literature provides a set of criteria to manage the redundancy such as the distance from singular positions, joint limits, dexterity and stiffness improvement [6,7,8].

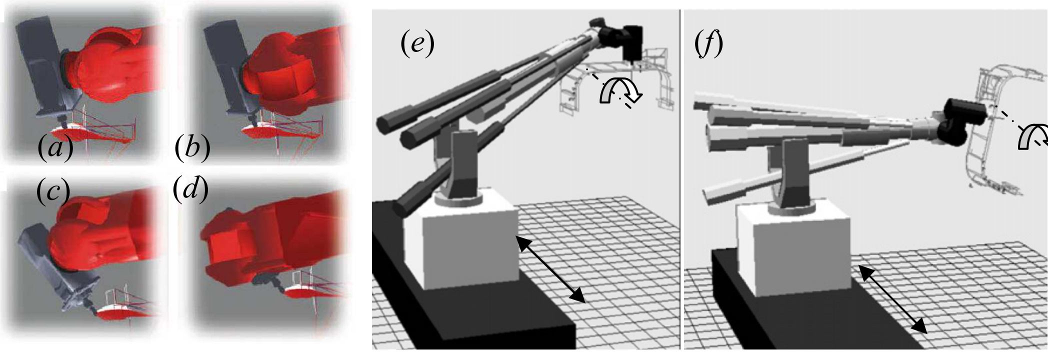

Figure 1: *Behavior improvement in the singularity position (a, b), optimal positioning regarding the task (c, d) [7]. Behavior improvement of a redundant robotic cell between pose without optimization (e) and optimized pose (f) [6].*

High speed machining (HSM)

HSM is the result of advances in the field of machining and is characterized by specific conditions. Various works on the topic have shown that an increase in the cutting speed gives rise to a specific decrease in cutting energy [9]. The work conditions improve the surface state, preserve material integrity and reduce cutting forces. However, these conditions generate constraints, such as increased spindle speed (N > 20000rpm), increased kinematic performance (V_f > 10m/min) and increased structural stiffness. HSM conditions, although more complex and more sensitive to settings, have to enable a good tool engagement. Moreover, it helps to satisfy the advance speed V_f to be as regular as possible equal to V_f imposed by the process.

Modeling of the redundant robotic cell

The task to be carried out has 5 dimensions characterized by the position of a point and the orientation of the tool axis. The degree of functional redundancy r_f is 1. This degree is represented by the angle of reorientation Δ of the effector around the tool axis (Fig. 2a). We integrate into the robotic cell a 2 axis rotary table. This 8-axis architecture has a degree of structural redundancy r_s equal to 2 represented by the two external controlled axes q_7 and q_8 (Fig. 2c). A TCS (Traveling Coordinate System) type model was created (Fig. 3) [9]. The parallelogram closed loop of the IRB6660 enhances both the accuracy and the load carrying capacity of the robot. The manipulator is composed of 9 joints and 9 links (Fig. 2b). We have 1 independent closed loop. The joints are either active or passive: 6 active joints $q=[q_1...q_6]$ equal to the number of the robot's degrees of freedom and 3 passive joints (q_{p1}, q_{p2}, q_{c1}).

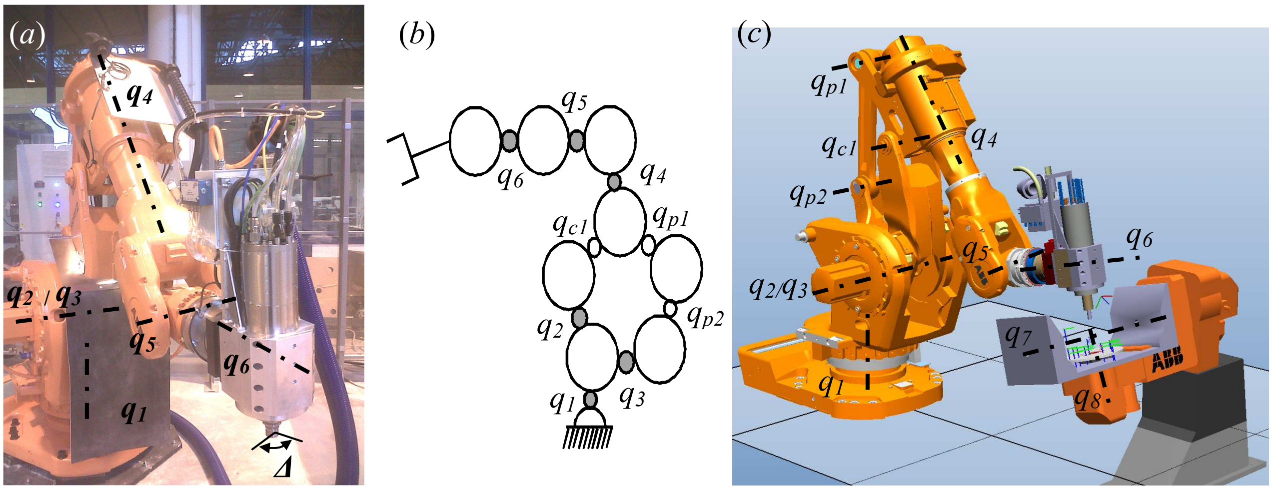

Figure 2: *Industrial robot IRB 6660 with HSM spindle (a), Architecture of IRB 6660 (b), representation of the redundant robotic cell (c)*

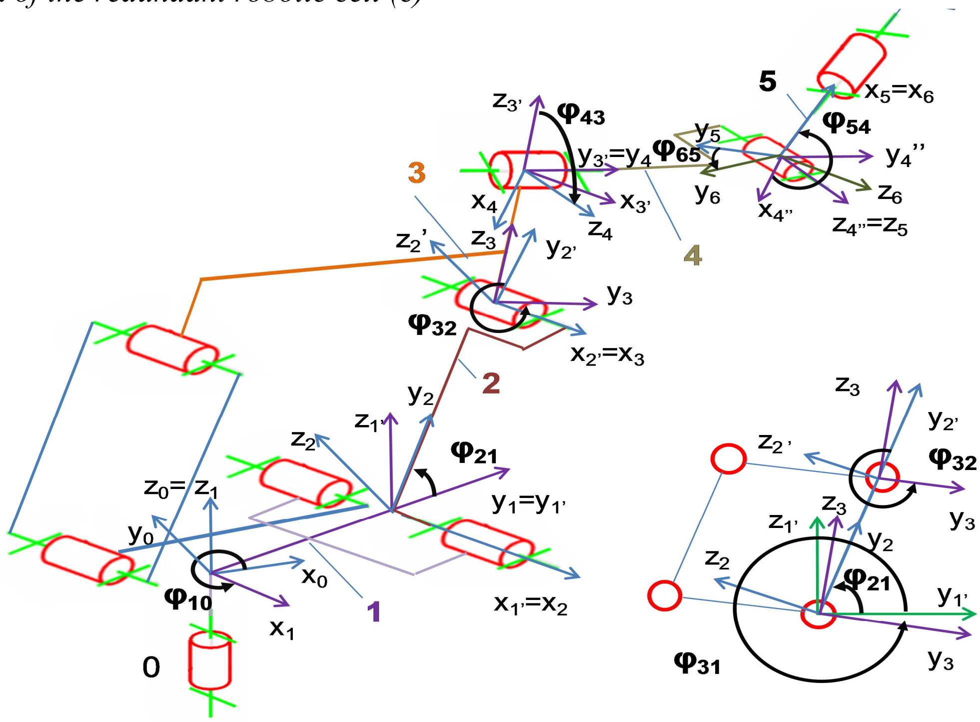

Figure 3: *Robotic structure diagram and the closed loop in the arm with the notation used in the TCS model [9]*

Direct Geometrical Model

The TCS direct geometrical model is represented by the following transformations from $O_0X_0Y_0Z_0$ to $O_6X_6Y_6Z_6$:

$$O_0X_0Y_0Z_0 \xrightarrow{R^z_{01}(\varphi_{10})} O_1X_1Y_1Z_1 \xrightarrow{T^y_{11'}(b_1)} O_{1'}X_{1'}Y_{1'}Z_{1'} \xrightarrow{R^x_{1'2}(\varphi_{21})} O_2X_2Y_2Z_2 \xrightarrow{T^y_{22'}(b_2)}$$
$$O_{2'}X_{2'}Y_{2'}Z_{2'} \xrightarrow{R^x_{2'3}(\varphi_{32})} O_3X_3Y_3Z_3 \xrightarrow{T^z_{33'}(b_3)} O_{3'}X_{3'}Y_{3'}Z_{3'} \xrightarrow{R^y_{3'4}(\varphi_{43})} O_4X_4Y_4Z_4 \xrightarrow{T^y_{44'}(a_4)} \quad (1)$$
$$O_{4'}X_{4'}Y_{4'}Z_{4'} \xrightarrow{R^z_{4'5}(\varphi_{54})} O_5X_5Y_5Z_5 \xrightarrow{R^x_{5'6}(\varphi_{65})} O_6\,X_6\,Y_6Z_6$$

A_{06} operator defining the pose of the end-effector is expressed as follows:

$$A_{06} = \underbrace{R^{z}_{01}(\varphi_{10}).T^{y}_{11'}(b_1)}_{A_{01}}.\underbrace{R^{x}_{1'2}(\varphi_{21}).T^{y}_{22'}(b_2)}_{A_{12}}.\underbrace{R^{x}_{2'3}(\varphi_{32})}_{A_{23}}.\underbrace{T^{z}_{33'}(b_3).R^{y}_{3'4}(\varphi_{43})}_{A_{34}}.\underbrace{T^{y}_{44'}(a4).R^{z}_{4'5}(\varphi_{54})}_{A_{45}}.\underbrace{R^{x}_{5'6}(\varphi_{65})}_{A_{56}} \quad (2)$$

Where

$$\varphi_{32} = \varphi_{31} - \varphi_{21} \quad (3)$$

Inverse Geometrical Model
To define the inverse geometrical model, we use the classical Paul's method. The pose U_0 of the end-effector and A_{06} are known. It consists in successively multiplying the two parts of the equation by the matrix A_{jj-1} (j will go from 1 to 5), to isolate and identify the different articular values.

Kinematic model
The kinematic model provides the velocity of the terminal link corresponding to the specified velocities of the active joints. As the joints of a tree structured robot are actuated and independent, the kinematic model for these robots can be obtained by applying the techniques developed for serial robots to each main branch. We first compute the kinematic model of the direct chain between the end effector and the base by proceeding as for a serial robot. With the various operators, the kinematic model is:

$$\begin{bmatrix} {}^{p}v \\ {}^{p}\omega \end{bmatrix}_h = \begin{bmatrix} {}^{p}J_h \end{bmatrix}\begin{bmatrix} \dot{q} \end{bmatrix} \quad (4)$$

${}^{p}v$ the translation velocity vector of the robot end-effector, expressed in the coordinate system p,
${}^{p}\omega$ the rotation velocity vector of the robot end-effector, expressed in the coordinate system p,
$\dot{q}$ the joint velocity vector composed of the relative velocities in the robot's kinematic pairs
$\begin{bmatrix} {}^{p}J_h \end{bmatrix}$ the Jacobian matrix
h the velocity reference point of the robot end effector.

With $h=p=3$, we obtain:

$$\begin{bmatrix} {}^{3}v \\ {}^{3}\omega \end{bmatrix}_3 = \begin{bmatrix} {}^{3}J_3 \end{bmatrix}\begin{bmatrix} \dot{q} \end{bmatrix} \text{ with } \begin{bmatrix} \dot{q} \end{bmatrix} = \begin{bmatrix} \dot{\varphi}_{10} & \dot{\varphi}_{21} & \dot{\varphi}_{32} & \dot{\varphi}_{43} & \dot{\varphi}_{54} & \dot{\varphi}_{65} \end{bmatrix} \quad (5)$$

$$\begin{bmatrix} {}^{3}v \\ {}^{3}\omega \end{bmatrix}_3 = \underbrace{\begin{bmatrix} -b_1 - b_2.C_{21} & 0 & 0 & -b_3 & a_4.C_{43} & -b_3.S_{54} - a_4.C_{54}S_{43} \\ 0 & b_2.S_{32} & 0 & 0 & b_3.C_{43} & b_3.C_{43}.C_{54} \\ 0 & b_2.C_{32} & 0 & 0 & -a_4.S_{43} & -a_4.C_{43}.C_{54} \\ 0 & 1 & 1 & 0 & S_{43} & C_{43}.C_{54} \\ S_{321} & 0 & 0 & 1 & 0 & S_{54} \\ C_{321} & 0 & 0 & 0 & C_{43} & -S_{43}.C_{54} \end{bmatrix}}_{\begin{bmatrix} {}^{3}J_3 \end{bmatrix}} \begin{bmatrix} \dot{\varphi}_{10} \\ \dot{\varphi}_{21} \\ \dot{\varphi}_{32} \\ \dot{\varphi}_{43} \\ \dot{\varphi}_{54} \\ \dot{\varphi}_{65} \end{bmatrix} \quad (6)$$

Where $C_{21}=cos(\varphi_{21})$, $S_{21}=sin(\varphi_{21})$, $C_{321}=cos(\varphi_{21}+\varphi_{32})$, $S_{321}=sin(\varphi_{21}+\varphi_{32})$, …

Equation 3 gives:

$$\dot{\varphi}_{32} = \dot{\varphi}_{31} - \dot{\varphi}_{21} \quad (7)$$

The Jacobian $\left[{}^{p}J_{h} \right]$ can be calculated by using the canonical or any other Jacobian of type $\left[{}^{e}J_{e} \right]$ [10]:

$$\left[{}^{p}J_{h} \right] = \begin{bmatrix} \left[a_{pe} \right] & \left[a_{pe} \right]\left[\wedge r_{he} \right] \\ 0 & \left[a_{pe} \right] \end{bmatrix} . \left[{}^{e}J_{e} \right]$$ where $A_{pe} = \begin{bmatrix} 1 & 0 \\ \left[r_{Oe} \right]_{p} & \left[a_{pe} \right] \end{bmatrix}$ and $\left[\wedge r_{he} \right]$ is the matrix of the cross product. (8)

Formalizing the optimization process

The problem of following trajectories with a redundant robot amounts to finding the parameters x which satisfy various constraints related to the task, the robot configuration and the capability expected. The problem can be expressed as:

Let $f : x \in \Re^{n} \to f(x) \in \Re^{k}$

Find $\left\{ x^{*} \right\}$ which minimizes $f^{i}(x)$ i = 1..k

Under $h : x \mapsto h(x) \leq 0$ and under $g : x \mapsto g(x) = 0$

Where n is the problem size and k is the number of criteria (9)

Criteria for redundancy management

Regarding the machining quality, the objective is to place the structure in the configuration which minimizes its deformation under the stress effect and allows greater capacity for the robot in terms of the end effector speed $V_f \geq V_f$ imposed in the advance direction d throughout the trajectory.

Kinematic criteria

The kinematic performance criteria of manipulators allow us to define the ability to move and to generate a particular speed from its current position. Dubey et al. [11] introduce two matrices W_x and W_q, positive and diagonal, which permit to split the relative influence of the end effector speed and the articular speed. The application allows us to define the values of W_x and W_q. If a preferred direction is expected from the end effector, W_x can be weighted. However, the advance direction d is modified by the performance of the robot represented by various criteria (accuracy, kinematic, joint limit, singularity) and the use of kinematic redundancy: W_x is therefore chosen as an identity matrix. However, to take into account the maximal speed of the articulation $\dot{q}_{i\max}$ (Fig. 7a), J_v is defined from the Jacobian matrix J as:

$$J_{v} = W_{x}^{1/2} J W_{q}^{-1/2} \quad \text{with} \quad W_{q}(i,i) = \frac{1}{\dot{q}_{i\max}^{2}} \quad \text{and} \quad W_{x}(i,i) = 1 \qquad \text{i=1..6} \tag{10}$$

We use a C_k criterion concerning the speed capacity given by [11]:

$$C_{k} = u_{d}^{T} (J_{v} J_{v}^{T})^{-1} u_{d} \tag{11}$$

with u_d a unit speed vector in the advance direction d. The robot's speed ratio R_k [11] is the ratio between the operational speed's norm $|\dot{x}|$ and the articular speed's norm $|\dot{q}_{v}|$:

$$R_k = \frac{|\dot{x}|}{|\dot{q}_v|} = \frac{|\dot{x}|}{|W_q.\dot{q}|} = \frac{1}{\sqrt{C_k}} \tag{12}$$

To highlight the importance of this criterion, results are presented in Fig. 5.

Criteria of joint limits

The joint limit criteria enable the joints to be used around their middle position q_{imoy}. A scalar function, whose effect is to increase the distance from the joint limit, enables the definition of a criterion C_q:

$$C_q = \sum_{i=1}^{6}\left(\frac{q_i - q_{imoy}}{q_{imoy} - q_{iM}}\right)^2 \quad \text{with } q_{iM} \text{ the maximum value of the axis} \tag{13}$$

Singularity avoidance criteria

In the robot's workspace, some positions exist where the end-effector loses one or several degrees of freedom called articular singularity obtained when the determinant of the Jacobian is zero.

$$-b_2.C_{54}.(b_3.C_{32} + a_4.S_{32}).(b_1 + a_4.C_{321} - b_3.S_{321} + b_2.C_{21}) = 0 \tag{14}$$

From eq. 14, 3 singular configurations can be defined

$$(b_1 + a_4.C_{321} - b_3.S_{321} + b_2.C_{21}) = 0 \tag{15}$$

$$(b_3.C_{32} + a_4.S_{32}) = 0 \tag{16}$$

$$C_{54} = 0 \tag{17}$$

Eq. 15 is associated with shoulder singularity where the first rotation axis passes by the wrist center point. In this singular configuration, 4 actuated revolute joints intersect at the same point. Fig. 4a shows that this singularity is outside of the workspace. Eq. 16 is associated with elbow singularity where a line intersects the joint axes (2, 3). Fig. 4b shows that this configuration is reached close to the workspace boundary. In this case, the criterion of joint limits (Eq. 13) is used to avoid this singularity. Eq. 17 defines wrist singularity where axes 4 and 6 are superposed. However, singularity avoidance may have a formulation similar to that of the avoidance of joint limits. The goal is to maximize the distance to the singular configuration. This criterion C_s with q_s designating the singular configuration can be written as:

$$C_s = \|q - q_s\| \tag{18}$$

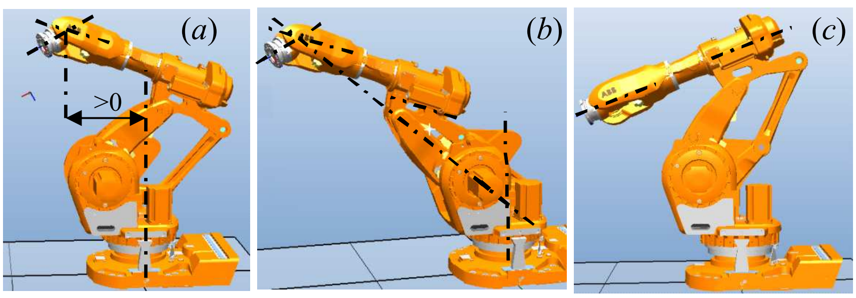

Figure 4: *Shoulder singularity cannot be reached in the workspace (a), elbow singularity (b), wrist singularity (c)*

Accuracy criteria

Many studies have considered that static deformations are mainly located in the joint [12,13,14]. According to Dumas et al. [14], the Cartesian stiffness matrix of a robot depends on its configuration, the stiffness of its components, its control and the stiffness of the axes. To simplify the problem, the elements are considered as non-shrinking elements and the study focuses on a small region of the workspace. Chen [15] defines the K_x cartesian stiffness matrix by the relation:

$$T = K_x.dX \tag{19}$$

T is a six-dimensional set composed of the forces and torques applied to the end effector. dX is a six-dimensional set composed of the translational and rotational displacements of the end effector. They are expressed in the robot frame. As K_θ, the joint stiffness matrix, is defined in a posture with good kinematic performance (dexterity) and away from the singular position, K_c, a complementary stiffness matrix is negligible [16] and K_x, the Cartesian stiffness matrix can be written as:

$$K_x = J^{-T}(K_\theta - K_c).J^{-1} \quad \text{with} \quad K_\theta(i,i) = k_{\theta_i} \quad i=1 \ldots 6 \quad \text{and} \quad Kc=[0] \tag{20}$$

A criterion C_{a1} is introduced to focus the displacement on the stiffest joints:

$$C_{a1} = \max\left(\sum_{i=1}^{6} \frac{k_{\theta i}}{\sum_{j=1}^{6} k_{\theta j}} q_i\right) \tag{21}$$

A criterion C_{a2} is also introduced related to the minimization of the cantilever of the robot in a simplified approach:

$$C_{a2} = \min\left|q_2 + q_3\right| \tag{22}$$

Resolution method

The optimization problem is solved by determining, for each pose, the angle Δ around the tool axis, q_7 and q_8 the axis position of the rotary table (Fig. 6). We use the classic method of solving redundancy by using the projection onto the kernel of the Jacobian matrix [6]:

$$\dot{q} = J^{+}\dot{x} + (\underbrace{I - J^{+}J}_{J_h})z \tag{23}$$

Where $J^{+} = J^{T}(JJ^{T})^{-1}$ is the pseudo-inverse of J, z is a vector of the same dimensions as q, I is the identity matrix (of dimension q) and J_h is the projection matrix of z on the kernel of J. Vector z in this case is defined as the gradient of an objective function C, constructed by aggregating the original objectives thus avoiding the construction of a Pareto front. One of the difficulties of aggregation methods is the choice of the weighting assigned to each criterion. To change the relative importance of each criterion according to the need, we use a method with variable weightings [17]. The form of the objective function becomes:

$$C(q) = \sum_{i=1}^{k} w_i(\overline{C}_i(x))(\overline{C}_i(q)) \quad \text{with} \quad \overline{C}_i(q) = \frac{C_i(q) - C_{i\min}}{C_{i\max} - C_{i\min}} \tag{24}$$

with $w_i(\bar{c}_i(q))$ the weighting function which depends on the criteria $\bar{c}_i$, which goes from 0 to 1.

Software integration

Models and resolution methods are computed under Matlab®. Part design and tool path generation are realized using CATIA® V5. We generate a file used by a 5-axis machine tool including tool end position and orientation. This file is readable by Matlab®. The software we develop with Matlab® allows us to generate and to test the trajectory, to optimize it and to see the influence of the parameters by integrating the various optimization criteria defined in this paper. RobotStudio® validates the results.

Simulation results

According to our constraints, the posture with the best performance needs to be found. As an example, Figure 5 presents the values of the normalized kinematic criteria R_{ky} while realizing the trajectory AB on the Y-axis, and the normalized accuracy criteria C_{a2} for the trajectory *AB*. It helps to understand how the robot's configuration affects the kinematic performances and the stiffness of the architecture. Moreover, the results show the conflicting goals of high feed rate V_f and high stiffness. This can be illustrated by the good kinematic behavior and low stiffness (Fig. 5c) and conversely (Fig. 5d).

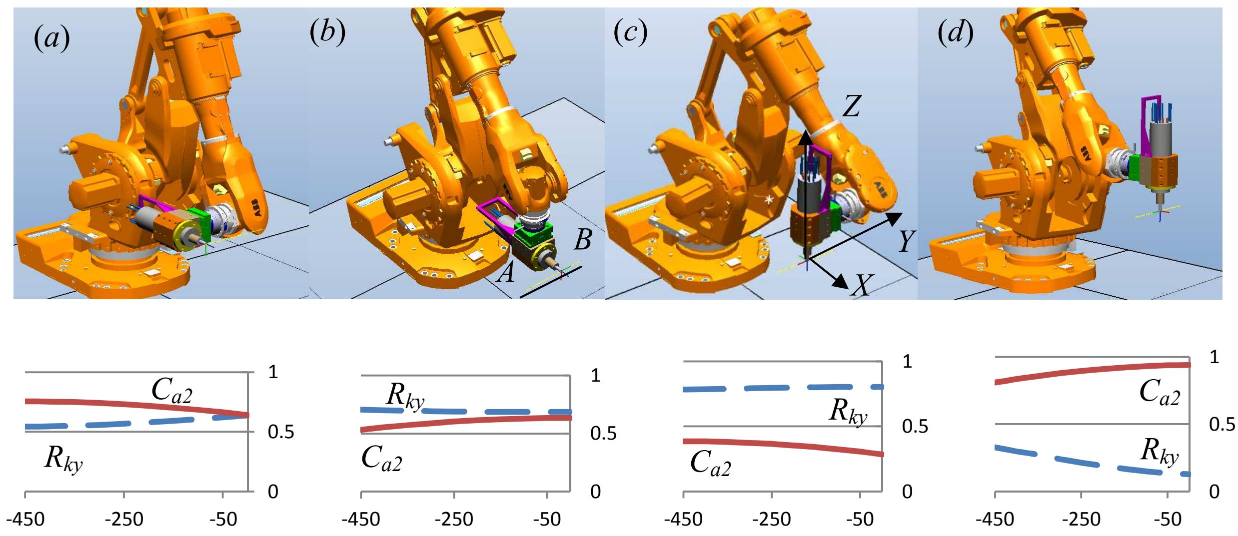

Figure 5: *Evaluation of the criterion R_{ky} and C_{a2} from A(1350,-450,750) to B(1350,0,750)*

These results present the advantages of working with a horizontal spindle [18]. In the case of the posture of Fig. 5a (posture 1), the main axes to cover the displacement are axes 1 and 5. For the posture of Fig. 5b (posture 2), the main axes are therefore 1 and 6. R_{ky} is higher in posture 2 because axis 6 is faster than axis 5 (Fig. 6a). Research on robot machining shows that stiffness is an important point to take into account when enhancing the accuracy and the quality of machined parts, and, in this respect, posture 1 seems to be the near-optimal configuration. So, in this configuration, a deeper study of dexterity needs to be undertaken. At point *A*, we realize a rotation around the axis tool and the evaluation of the kinematic criteria is done on the displacement on the *Y*- and *Z*-axes. The result presents good kinematic behavior for an angle α equal to 45°. The stiffness study will therefore be realized in this configuration. Focusing on the main criteria (kinematic and cantilever), this first result allows us to define an acceptable location for our rotary table. The stiffness study in the configuration in Fig. 6 and the realization of machining parts will allow us to evaluate the efficiency of the optimization and the defined criteria.

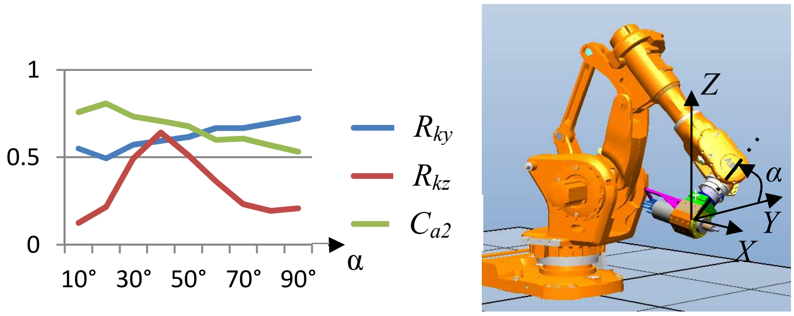

Figure 6: *Optimal kinematic configuration to define articular stiffness*

(a)

Axis	max speed
$\dot{q}_1$	130°/s
$\dot{q}_2$	130°/s
$\dot{q}_3$	130°/s
$\dot{q}_4$	150°/s
$\dot{q}_5$	120°/s
$\dot{q}_6$	190°/s

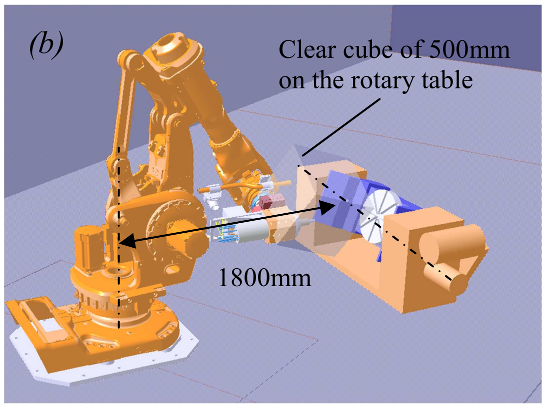

Figure 7: *Maximum axis speed (a) - Final configuration of the robotic cell (b)*

Conclusion

This work focuses on the evaluation of the robotic performance dedicated to a machining task. The main aim is to define a good location for the rotary table taking into account various criteria and the spindle environment. This requires prior characterization of the geometric, kinematic and dynamic behavior. By studying kinematic performances and robot's cantilever, we define the posture to analyze the stiffness. A good location of the rotary table is also presented. This architecture allows us to machine parts while the robot is working in a space with pre-defined performance. Trials on aluminum parts will allow validation of the criteria used during optimization and verification of the performance we can expect of such a redundant robotic cell.

Acknowledgements

We acknowledge the financial support for this work in the frame of InnovaPole project funded by Region Council of Auvergne and FEDER.

References

[1] Z. Pan, H. Zhang, Z. Zhu, J. Wang, Chatter analysis of robotic machining process , J. of materials processing technology, 173 (2006) 301-309.

[2] H. Zhang, J.Wang, G. Zhang, Z.Gan, Z.Pan, H.Cui, Z.Zhu, Machining with flexible manipulator: toward improving robotic machining performance, in: IEEE/ASME Int. Conf. on, California, 2005, pp. 1127-1132.

[3] A. Mohan, S. P. Singh, S. K. Saha, A cohesive modeling technique for theoretical and experimental estimation of damping in serial robots with rigid and flexible links, Multibody system dynamic, 23 (2010), 333-360.

[4] M. Cherif, J.-Y. K'nevez, A. Ballu, Thermal effects on robot machining accuracy, in: IDMME Bordeaux, 2010.

[5] M. Summers, Robot capability test and development of industrial robot positioning system for the aerospace industry , SAE transactions, 114 (2005) 1108-1118.

[6] V. Robin, L. Sabourin, G. Gogu, Optimization of a robotized cell with redundant architecture, Robotics and Computer-Integrated Manufacturing 27 (2011) 13-21.

[7] W. Xiao, H. Straub, T. loohb, Closed-form inverse kinematics of 6R milling robot with singularity avoidance, Prod. Eng. Res. Devel., 2010.

[8] C. Tournier, High Speed Machining. Dunod, 2010.

[9] G. Gogu, P. Coiffet, A. Barraco, Representation of robots displacements, Paris: Hermès, 1997.

[10] G. Gogu, P. Coiffet, Structural synthesis of anthropomorphic robotic manipulators with only isolated singularities, in: Proceedings of 35th International Symposium on Robotics, Paris, 2004.

[11] R. Dubey, J. Y. S. Luh, Redundant robot control using task based performance measures, Journal of robotic systems, 5 (1988) 409-432.

[12] A. Olabi, R. Béarée, O. Gibaru, M. Damak, Feedrate planning for machining with industrial six-axis robots, Control Engineering Practice, 18 (2010) 471-482.

[13] E. Abele, M. Weigold, et S. Rothenbücher, Modeling and Identification of an Industrial Robot for Machining Applications, in: General Assembly of CIRP N°57, Dresden, 2007, pp.387-390.

[14] C. Dumas, S. Caro, S. Garnier, et B. Furet, Joint stiffness identification of six revolute industrial serial robots, Robotics and Computer-Integrated Manufacturing, 27 (2011) 881-888.

[15] S.-F. Chen, The 6x6 stiffness formulation and transformation of serial manipulators via the CCT theory, in: IEEE International Conference on Robotics & Automation, Taiwan, 2003.

[16] G. Alici, B. Shirinzadeh, Enhanced Stiffness Modeling, Identification and Characterization for Robot Manipulators 21 (2005) 554-564.

[17] K.-kyu Lee, M. Buss, Redundancy resolution with multiple criteria, in: Intelligent Robots and Systems,in: IEEE/RSJ Int. Conf. on, Beijing, 2006, pp. 598-603.

[18] Wang, J., Zhang, H., Fuhlbrigge, T., 2009. Improving machining accuracy with robot deformation compensation, in: IEEE/RSJ Int. Conf on. Intelligent Robots and Systems, St-Louis, 2009, pp. 3826-3831.